

Electronic supplementary information for

Dynamic Spatial and Structural Organization in Artificial Cells Regulates Signal Processing by Protein Scaffolding

Bastiaan C. Buddingh', Antoni Llopis-Lorente, Loai K. E. A. Abdelmohsen*, Jan C. M. van Hest*

Department of Chemical Engineering and Chemistry, Institute for Complex Molecular Systems & Department of Biomedical Engineering, Eindhoven University of Technology, PO Box 513, 5600 MB Eindhoven, the Netherlands. E-mail: J.C.M.v.Hest@tue.nl; L.K.E.A.Abdelmohsen@tue.nl.

Experimental Procedures

Materials

Nano-Glo Luciferase Assay Substrate (furimazine solution) was obtained from Promega. Phospholipids were supplied by Avanti Polar Lipids. Paraffin oil (0.86 g/cm³ at 20 °C) was from JT Baker. Urease from *Canavalia Ensiformis* (40 U/mg solid), Proteinase K from *Engyodontium album* and alpha-hemolysin (αHL) from *Staphylococcus aureus* were purchased from Sigma-Aldrich. The dextran-fluorescein-tetramethylrhodamine conjugate (70,000 g/mol, anionic) was obtained from Thermo Fisher Scientific. All other reagents and solvents were of high-quality grade, purchased from commercial suppliers, and used without further purification unless stated otherwise. Ultrapure water ("Milli-Q") was obtained from a Merck Millipore Q-Pod system (≥ 18.2 MΩ) with a 0.22 μm Millipore Express 40 filter.

Lipids used throughout this study: 1,2-dioleoyl-*sn*-glycero-3-phosphocholine (DOPC), 1,2-dioleoyl-*sn*-glycero-3-phosphoethanolamine-*N*-(lissamine rhodamine B sulfonyl) (DOPE-LRB), 1-palmitoyl-2-oleoyl-glycero-3-phosphocholine (POPC), 1,2-dioleoyl-*sn*-glycero-3-[(*N*-(5-amino-1-carboxypentyl)iminodiacetic acid)succinyl] (nickel salt) (DOGS-NTA-Ni), 1,2-distearoyl-*sn*-glycero-3-phosphoethanolamine-*N*-[biotinyl(polyethylene glycol)-2000] (DSPE-PEG).

Instrumentation

Bulk fluorescence measurements were obtained using either a Spark 10 M, Safire 2, or Infinite 200 PRO plate reader (Tecan). Bioluminescence spectroscopy was recorded on a Tecan Spark 10 M. Sonication was performed in a Branson 2800 or 2510 bath ultrasonic cleaner. Images were processed with Fiji, a program developed by the NIH and available as public domain software at <https://imagej.net/Fiji>. Bioluminescence microscopy was performed on a Nikon Eclipse Ti-e inverted microscope equipped with a Plan Apo Lambda 20x objective (Nikon). To prevent lipid adsorption to the glass, slides were treated with 1 mg/ml BSA in Milli-Q for >1 h, followed by washing with Milli-Q.

Procedures

All experiments were performed at room temperature, unless indicated otherwise. All enzyme solutions were kept on ice during the procedures, whenever possible.

Protein expression & characterization: LgBiT was expressed as a fusion protein (His₆-LgBiT-(GGG)₁₀-CT52) as reported previously.¹ The CT52 domain was not used in the current study. tdTomato was expressed with an N-terminal His-tag as described previously.²

Solid-phase peptide synthesis: The His-tagged and untagged SmBiT fragments were synthesized by SPPS. Peptides were synthesized by standard automated Fmoc-SPPS (Intavis MultiPep RSi) using Tentagel S RAM resins. The Fmoc-protected amino acid building blocks (4 eqv.) were dissolved in DMF and coupled sequentially to the resin using DIPEA (8 eqv.), and HBTU (4 eqv.) for 30 min. Each amino acid coupling was repeated once to increase conversion. After double coupling, a single capping step was performed using 20 vol% acetic anhydride, 20 vol% pyridine in DMF to terminate any uncoupled chains. Fmoc deprotection was performed twice using 20 vol% piperidine in DMF for 5 min each.

The peptides were cleaved from their resin using 1.5 ml of 81.5% TFA, 5% thioanisole, 5% phenol, 5% water, 2.5% EDT, 1% TIS (vol%) per 100 mg resin for 2.75 h, followed by filtration and washing of the resin with TFA. The filtrates were precipitated into ice-cold diethyl ether, stored at -20 °C for 15 min, and centrifuged at 2,000 rpm for 10 min (MSE Mistral 1000 centrifuge). The supernatants were decanted and the pellets were washed with fresh ice-cold ether, and centrifuged again. This washing was repeated once. The pellets were dried under vacuum overnight and purified by preparative RP-HPLC using a gradient of 5–100% MeCN in H₂O + 0.1% TFA. Both products were obtained after lyophilization as a white powder.

The (His-)SmBiT fragment consisted of an N-terminal His-tag, a GGS-linker and the 11-amino acid small fragment of NanoBiT: H-HHHHHHGGSGGGGSGGSSSGGVTGYRLFEEIL-NH₂. LC-MS (ESI+): m/z calcd. for C₁₃₄H₁₉₆N₄₈O₄₃ [M+3H]³⁺: 1056.5, observed: 1056.5; LC: R_t = 6.31 min.

The NoHis-SmBiT fragment consisted of the GGS-linker with the small fragment of NanoBiT: H-GGSGGGGSGGSSSGGVTGYRLFEEIL-NH₂. LC-MS (ESI+): m/z calcd. for C₉₈H₁₅₄N₃₀O₃₇ [M+2H]²⁺: 1173.1, observed: 1173.1; LC: R_t = 6.53 min.

Assembly of GUVs: GUVs were prepared following the droplet transfer method.³ First, lipid stock solutions in paraffin oil were prepared by mixing lipid stock solutions in chloroform with paraffin oil, heating this to 80 °C for 30–60 min and leaving it under vacuum overnight. These solutions were stored at -20 °C and used within two weeks. Paraffin stock solutions were mixed to obtain 200 μl of a solution containing either 70/30 (mol/mol) POPC/cholesterol, 35/35/30 DOPC/POPC/cholesterol or 100% DOPC. To obtain Ni-NTA-displaying GUVs, 1 or 2% of DOGS-NTA-Ni was added. When membrane labeling was needed, 0.06% of DOPE-LRB was incorporated as well. The lipid solutions were sonicated at room temperature for 10 min in a bath sonicator and cooled on ice for >15 min. Next, 20 μl of inner phase solution (*vide infra*) was emulsified in 200 μl of lipid solution by strong vortexing for 25 s while turning the reaction tube to prevent sedimentation of the water droplet. Directly after, the emulsions were incubated on ice for 10 min. Subsequently, they were layered on top of 150 μl pre-cooled outer phase solution (*vide infra*) in a 1.5 ml plastic reaction tube and immediately centrifuged at 4 °C for 20 min at 3,300 × g (standard) or at room temperature at 9,000 × g (POPC/cholesterol GUVs). GUVs were harvested by puncturing the tube at the position of the GUV pellet and collecting the aqueous layer. Either 2 mM EDTA was added to the solution to prevent binding of unencapsulated proteins, or the GUVs were carefully washed to remove unencapsulated material by two steps of centrifugation at 1,500 × g for 2 min and replacement of the supernatant.

Inner phase compositions: 10 mM K₂HPO₄, 300 mM NaCl, 200 mM sucrose, 5.0 μM LgBiT, 5.0 μM SmBiT or NoHis-SmBiT, pH 7 or 5. Where applicable, 10–100 μM of sulforhodamine B (SRB) or calcein was added to track the position of the GUVs or to normalize for the concentration of GUVs.

Outer phase compositions: 10 mM K₂HPO₄, 300 mM NaCl, 200 mM glucose, pH 7 or 5.

The pH of the inner phase and outer phase was set at room temperature using a potentiometric pH meter. All components were mixed and small volumes of NaOH or HCl were added to attain the desired pH. Next, the total volume was adjusted with Milli-Q to reach the desired volume.

Bioluminescence spectroscopy: Measurements were performed in a white, low-volume 384-well microplate with non-binding surface treatment (Corning) at 25 °C. 20 µl of GUV solution was mixed with 2.0 µl diluted Nano-Glo substrate (final concentration 1:220). Immediately afterwards, the plate was shaken for 15 s and the measurement was started. Luminescence was collected using an integration time of 200 or 5000 ms (depending on the NanoBiT concentration); the luminescence was recorded with an interval of 1 min until a stable output was reached, which was used for quantification. For each sample the bioluminescent signal was normalized to the fluorescence of encapsulated sulforhodamine B or calcein to account for the GUV concentration.

Bioluminescence microscopy: Bioluminescence microscopy was performed on a Nikon Eclipse Ti-e inverted microscope equipped with a Plan Apo Lambda 20x objective (Nikon). The GUVs were loaded into a BSA-passivated 8-well µslide with a #1.5 glass coverslip bottom (Ibidi). Nano-Glo substrate was added, diluting either 1:50 or 1:100, and directly afterwards the bioluminescent signal was collected using an Andor iXon Ultra 888 EMCCD camera with an operating temperature of -80 °C, an integration time of 60 s, and the electron multiplier gain set to 234. Bioluminescence was collected over several minutes until a stable signal was obtained. To localize the GUVs, the fluorescent signal from fluorophores located either in the lumen or the membrane of the vesicles was recorded using a bandpass filter set with either excitation at 460–500 nm, a 505 nm dichroic mirror and emission filter at 510–560 nm (calcein), or excitation at 540–580 nm, a 585 nm dichroic mirror, and emission at 592–667 nm (DOPE-LRB, sulforhodamine B). To track the pH inside the GUVs, the ratiometric fluorescent pH probe dextran-fluorescein-tetramethylrhodamine (dextran-FT) was employed using the aforementioned filter set.

Confocal laser scanning microscopy: Confocal microscopy was performed on a Leica TCS SP8 microscope. The GUVs were loaded into a BSA-passivated 8-well µslide with a #1.5 glass coverslip bottom (Ibidi). For images displayed in **Suppl. Fig. 19**, tdTomato was excited at 552 nm and emission was collected at 560–620 nm using a HC PL APO CS2 63x/1.20 water immersion objective. For time-lapse datasets shown in **Suppl. Fig. 21**, fluorophores were excited sequentially; fluorescein was excited at 488 nm and emission was collected at 495–540 nm; tetramethylrhodamine was excited at 552 nm and emission was collected at 565–610; a HC PL APO CS2 20x/0.75 dry objective was used. 2x line averaging was applied for image acquisition and the settings were not change during the experiment to allow direct comparison of the fluorescence intensities.

Image analysis: Micrographs were analyzed using Fiji. To quantify the spatial organization and activation of NanoBiT, the bioluminescent signal both at the membrane and in the lumen was extracted using the radial profile extended plug-in developed by Philippe Carl at the University of Strasbourg.⁴ GUVs were analyzed individually, and the integration angle was adjusted to avoid regions where GUVs had clustered. Examples of the resulting radial profile plots are displayed in **Suppl. Fig. 10**. From the bioluminescent signal at the membrane and in the lumen of the GUVs, the membrane/lumen ratio of bioluminescence was calculated to quantify the spatial organization and activation of NanoBiT.

Conditions per experiment

Spatial organization and activation of NanoBiT, Figure 2a: GUVs were loaded with 5 μM SmBiT and 5 μM LgBiT. The membrane composition was 70/30 (mol/mol) POPC/cholesterol + 1% DOGS-NTA-Ni. The pH of both inner and outer phase was 7.4. The final dilution of Nano-Glo substrate was 1:50. **Figure 2b:** GUVs were loaded with 10 μM sulforhodamine B and varying concentrations of SmBiT and LgBiT, as indicated in the figure. The membrane composition was 35/35/30 (mol/mol) DOPC/POPC/cholesterol + 1% DSPE-PEG + 0 or 2% DOGS-NTA-Ni. The pH of both inner and outer phase was 7.4. The final dilution of Nano-Glo substrate was 1:220. The global bioluminescent signal was normalized to the GUV concentration using the fluorescence of encapsulated sulforhodamine B. **Figure 2c:** GUVs were loaded with 5 μM of either His-SmBiT or NoHis-SmBiT, 5 μM LgBiT, and 100 μM calcein. The membrane composition was 35/35/30 (mol/mol) DOPC/POPC/cholesterol + 1% DSPE-PEG (for improved GUV production) + 2% DOGS-NTA-Ni. The pH of both inner and outer phase was 7.4, and 2 mM EDTA was added to the external solution. The final dilution of Nano-Glo substrate was 1:50. The global bioluminescent signal was normalized to the GUV concentration using the fluorescence of encapsulated calcein.

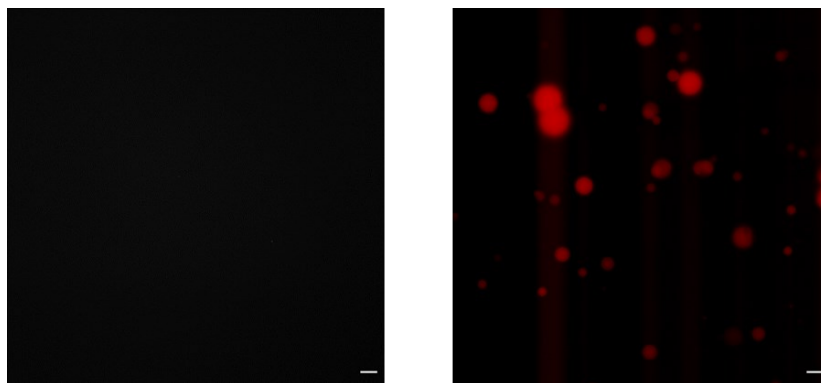
pH-dependent spatial organization, Figure 3: GUVs were loaded with 5 μM LgBiT and 5 μM SmBiT. The membrane composition was 35/35/30 (mol/mol) DOPC/POPC/cholesterol + 0.06% DOPE-LRB + 1% DSPE-PEG + 1% DOGS-NTA-Ni. αHL (20 $\mu\text{g}/\text{ml}$) was added and incubated for 20 min to form membrane pores in the GUVs. The pH of all solutions was monitored using a potentiometric pH meter. At the start, the pH of both inner and outer phase was 7.4. Three series of samples were prepared: one was left untreated (pH 7.4), to another dilute HCl was added to decrease the pH to 5.5, yet another was first acidified (pH 5.5) and after 20 min incubation adjusted to pH 7.5 using dilute NaOH. Next, Nano-Glo substrate (1:50 final dilution) was added and the bioluminescence recorded. In this case, EDTA was not added to the external solution, as it would have diffused into the GUVs and inhibited the membrane recruitment of the internal protein fragments as well.

Urease/urea-controlled enzymatic signaling, Figure 4: GUVs were loaded with 5 μM LgBiT, 5 μM SmBiT, 100 U/ml urease and 0.1 mg/ml dxFT. The membrane composition was 35/35/30 (mol/mol) DOPC/POPC/cholesterol + 0.06% DOPE-LRB + 0.5% DSPE-PEG + 2% DOGS-NTA-Ni. Here, the buffer composition was 20 NaOAc, 150 mM NaCl and 200 mM sucrose (inner phase) or glucose (outer phase), and the GUVs were washed twice by centrifugation. Next, αHL (20 $\mu\text{g}/\text{ml}$) was added and incubated for 20 min to form membrane pores in the GUVs, followed by addition of Proteinase K (70 $\mu\text{g}/\text{ml}$) to inactivate any unencapsulated NanoBiT. The pH of all solutions was monitored using a potentiometric pH meter. At the start, the pH of both inner and outer phase was 7.5. Three series of samples were prepared: one was left untreated (pH 7.5), to another dilute HCl was added to decrease the pH to 5.5, yet another was first acidified (pH 5.5) and after 20 min of incubation urea was added (final concentration 40 mM). The change of the internal pH was followed by time-lapse fluorescence microscopy using the ratiometric pH probe dextran-FT. Upon stabilization of the pH, Nano-Glo substrate (1:100 final dilution) was added and the bioluminescence recorded.

Supplementary Figures and Tables

Supplementary Figure 1.

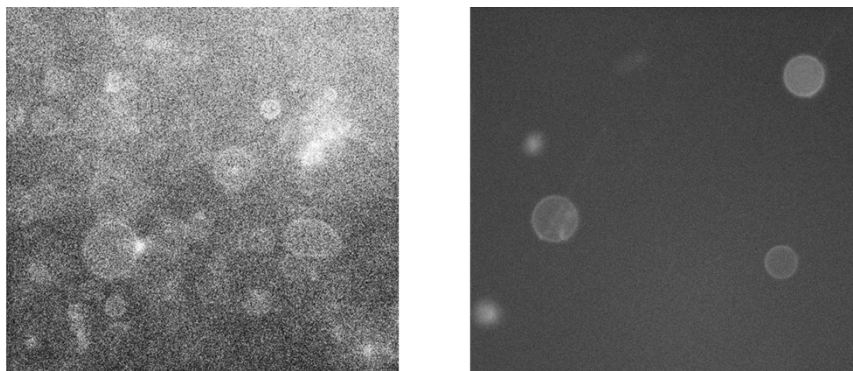
In absence of furimazine, no bioluminescence is produced.



Negative controls for bioluminescent signal in absence of furimazine, the substrate for NanoBiT. Micrographs display bioluminescence (left) and fluorescence from a marker in the lumen of the GUVs (calcein; right). GUVs contained 5 μM LgBiT and SmBiT and the pH was 7.4. 2.0 mM EDTA was present in the external solution. Scale bars represent 30 μm .

Supplementary Figure 2.

>1 μM of LgBiT and SmBiT is needed for adequate signal/noise ratio in bioluminescence imaging.

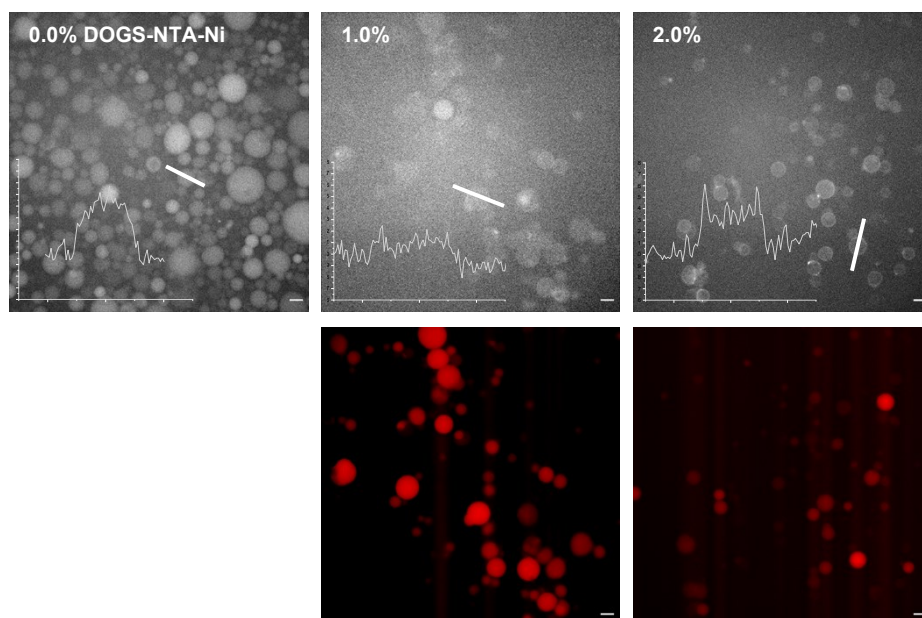


Bioluminescence micrographs for GUVs that contained 1 μM (left) or 5 μM (right) LgBiT and SmBiT. GUVs contained 2% DOGS-NTA-Ni and the pH was 7.

The limit of detection for the bioluminescence microscopy required the GUVs to be loaded with at least 5 μM of both LgBiT and SmBiT to collect sufficient photons. At this concentration some spontaneous, Ni-NTA-independent reconstitution of the two luciferase fragments occurred, which is the cause for the luminescent signal that was observed in the lumen of the vesicle without DOGS-NTA-Ni in **Figure 2a**.

Supplementary Figure 3.

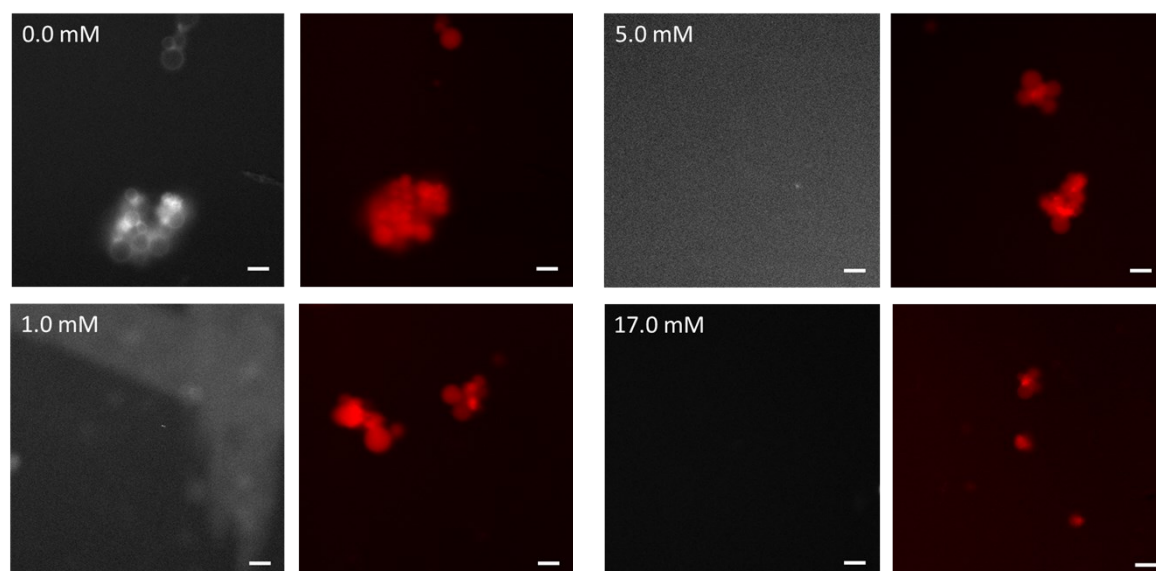
The amount of DOGS-NTA-Ni in the GUV membrane controls LgBiT and SmBiT binding.



Micrographs of bioluminescence (upper row) and a GUV marker (calcein; lower row) of GUVs containing different concentrations (in mol%) of DOGS-NTA-Ni. GUVs were loaded with 5 μ M LgBiT and SmBiT and the pH was 7.4. 2.0 mM EDTA was present in the external solution. Scale bar represents 20 μ m. The Nano-Glo substrate was diluted 1:50. The graphs show the line profiles of the GUVs indicated by the white lines.

Supplementary Figure 4.

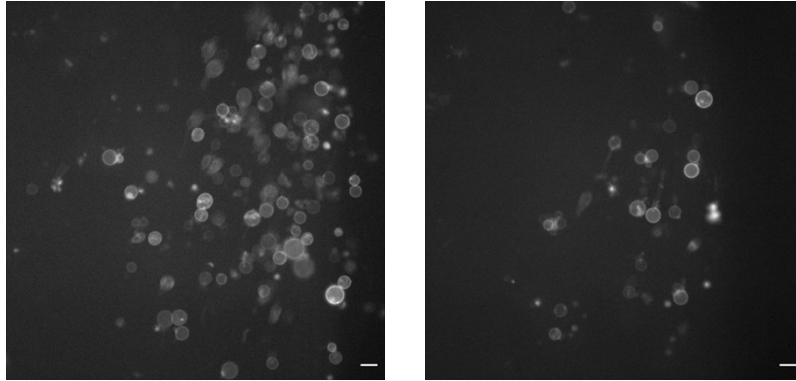
EDTA removes NanoBiT from the membrane of GUVs that contain DOGS-NTA-Ni.



Micrographs of bioluminescence (gray) and a GUV marker (dextran-FITC-TMR conjugate; red). In this case, LgBiT and SmBiT ($0.50 \mu\text{M}$) were added to the external solution after GUV formation. GUVs contained 1% DOGS-NTA-Ni and the pH was 7.4. After allowing both NanoBiT fragments to bind the GUVs for 20 min, EDTA was added at the indicated concentration. Nano-Glo substrate (1:50 final dilution) was added 20 min after starting EDTA incubation. Scale bar represents $20 \mu\text{m}$.

Supplementary Figure 5.

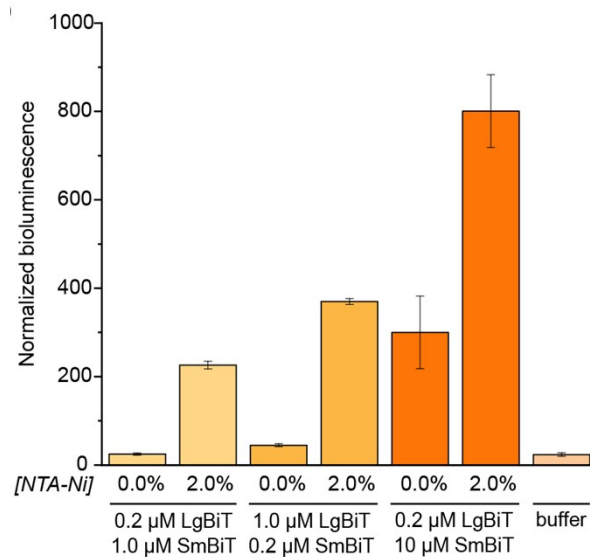
EDTA does not inhibit the recruitment of NanoBiT inside the vesicles.



Bioluminescence micrographs from GUVs that contained 5 μ M LgBiT and SmBiT. GUVs contained 2% DOGS-NTA-Ni and the pH was 7.4. EDTA was added to the external solution at 1.0 mM (left) or 2.0 mM (right). Nano-Glo substrate was diluted 1:50. Scale bars represent 30 μ m. This demonstrates that the EDTA that was added to the external solution does not leak into the GUVs, and that the observed bioluminescence originates from the internal reconstituted NanoBiT (compare with **Suppl. Fig. 4**).

Supplementary Figure 6.

The influence of fragment concentration and stoichiometry on global bioluminescence output.

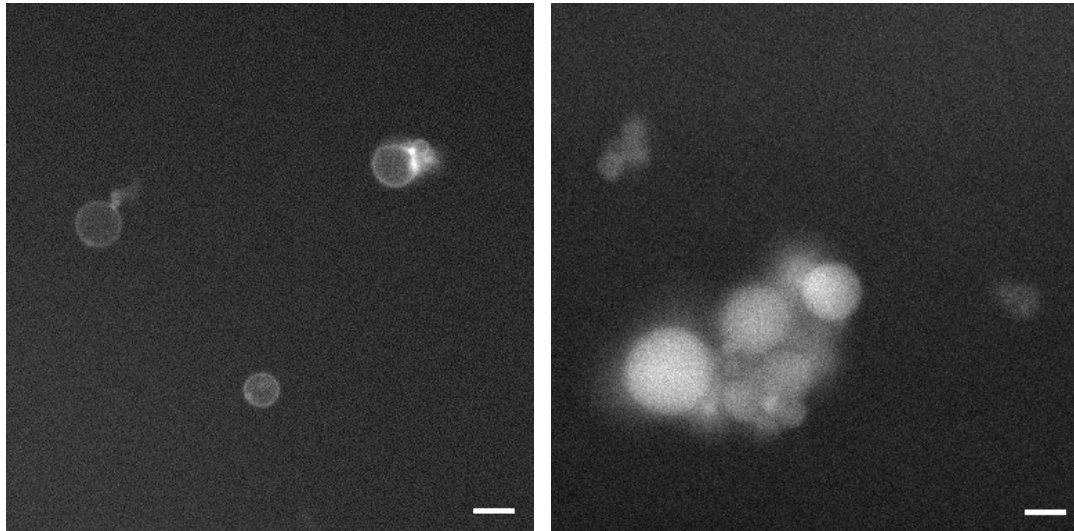


Bioluminescence of GUVs with or without 2% DOGS-NTA-Ni and varying concentrations of encapsulated LgBiT and SmBiT. The bioluminescence was normalized to the number of GUVs. All experiments were performed at pH 7.4. Error bars denote standard deviation.

The absolute bioluminescent signal depended on the concentration of both fragments inside the vesicles; the stoichiometry of the interaction was unimportant, but – as expected – higher concentrations of LgBiT and SmBiT produced higher enzymatic activity. At low concentrations of both fragments (0.2 and 1.0 μM), the bioluminescent signal in artificial cells without DOGS-NTA-Ni-mediated spatio-structural organization was negligible, whereas organization of the complex at the membrane induced an increase of the signal of up to one order of magnitude.

Supplementary Figure 7.

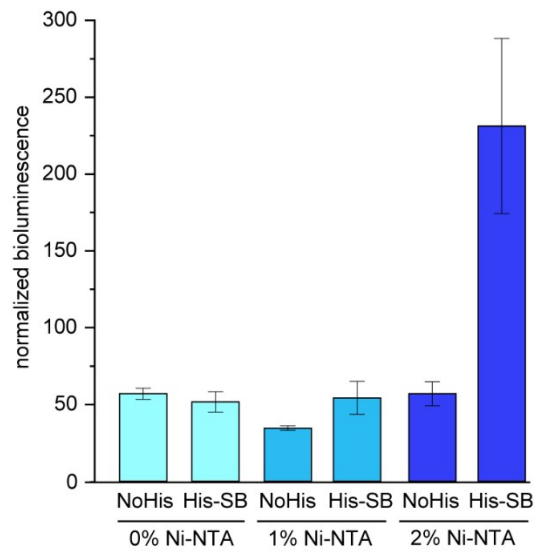
Full fields of view for the experiment displayed in Figure 2.



Bioluminescence micrographs of GUVs containing 1% DOGS-NTA-Ni (left) or 0% DOGS-NTA-Ni (right). 5 μ M LgBiT and 5 μ M SmBiT were encapsulated and the pH was 7.4. Scale bars represent 20 μ m.

Supplementary Figure 8.

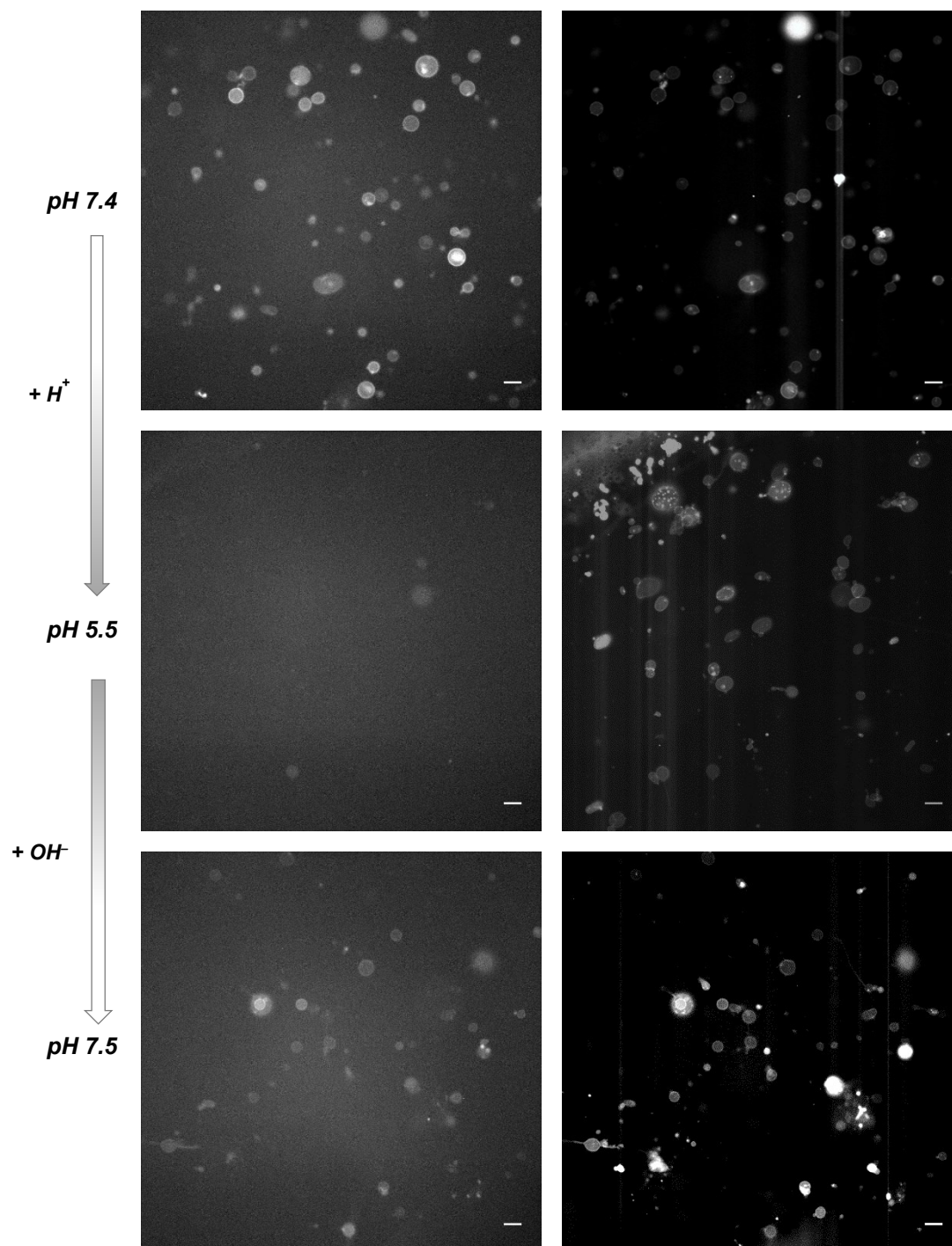
The effect of SmBiT recruitment to the membrane on enzyme reconstitution.



Global bioluminescence of samples with GUVs containing LgBiT (5 μM) and either His-SmBiT or NoHis-SmBiT (5 μM). The GUVs were functionalized with 0, 1 or 2% DOGS-NTA-Ni. 2 mM EDTA was added to the external solution. The bioluminescence was normalized to the number of GUVs. All experiments were performed at pH 7.4. Error bars denote the standard deviations.

Supplementary Figure 9.

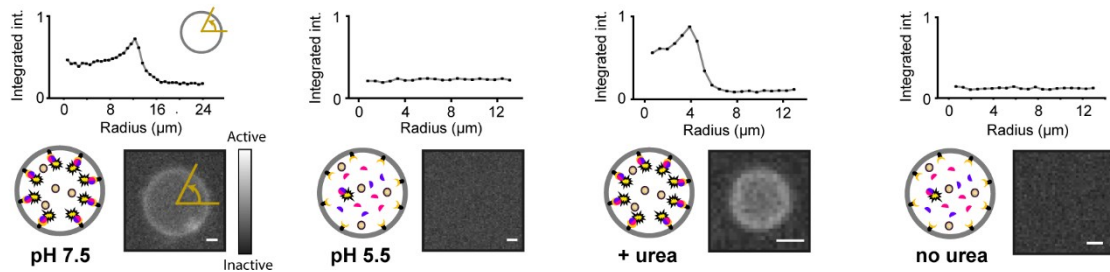
Full fields of view for the experiment displayed in Figure 3.



Bioluminescence (left) and fluorescence (right) micrographs. The fluorescent lipid DOPE-LRB was incorporated into the membrane of the GUVs to mark their positions. The GUVs contained 1% DOGS-NTA-Ni, 0.06% DOPE-LRB, 5 μ M LgBiT and 5 μ M SmBiT. Scale bars represent 30 μ m.

Supplementary Figure 10.

Radial profile plots of bioluminescent GUVs



As described in the Experimental Procedures, to quantify the spatial organization and activation of NanoBiT, the bioluminescent signal both at the membrane and in the lumen was extracted using the radial profile extended plug-in developed by Philippe Carl at the University of Strasbourg.⁴

This plug-in produces a profile plot of normalized integrated intensities around concentric circles as a function of distance from the center of the GUV. The plug-in sums the pixel intensities of the concentric rings and normalizes for the number of pixels, yielding normalized integrated intensities.

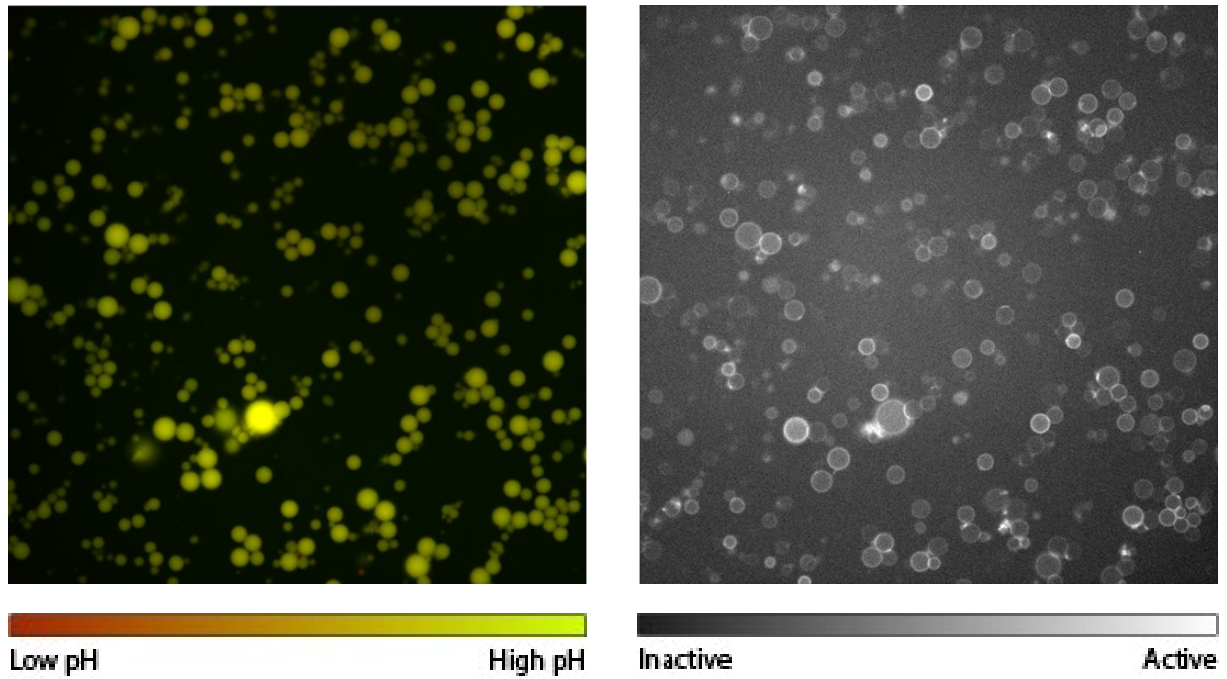
GUVs were analyzed individually, and the integration angle (indicated by the brown arrow) was typically 360° – unless to avoid regions where GUVs had clustered.

From the bioluminescent signal at the membrane and in the lumen of the GUVs, the membrane/lumen ratio of bioluminescence was calculated to quantify the spatial organization and activation of NanoBiT (see **Fig. 4c**).

This figure shows the radial profiles of four representative GUVs above their respective bioluminescence micrographs. The center of each GUV is located at radius = 0 μm.

Supplementary Figure 11.

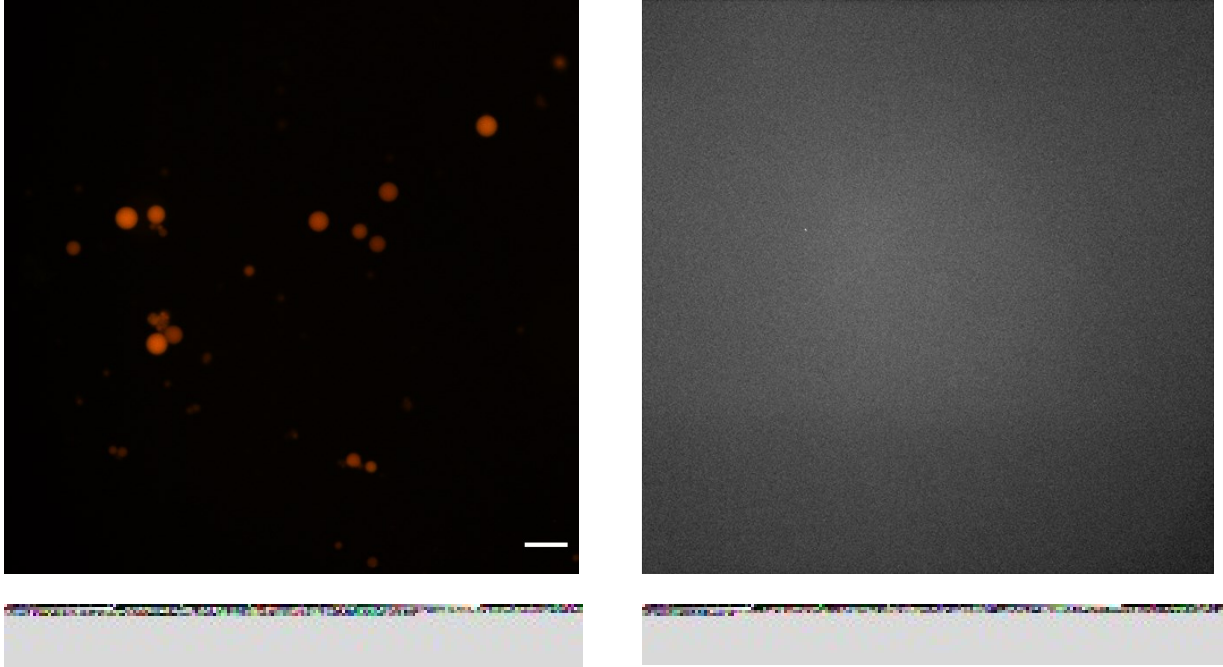
Full fields of view for the experiment displayed in Figure 4; at the start (pH 7.5).



Micrographs of the fluorescent signal from the pH probe (left) and bioluminescent signal from the reconstituted NanoBiT (right). The GUVs contained 2% DOGS-NTA-Ni, 5 μ M LgBiT, 5 μ M SmBiT, 100 U/ml urease and 0.1 mg/ml dextran-FT (pH probe) and were prepared at pH 7.5.

Supplementary Figure 12.

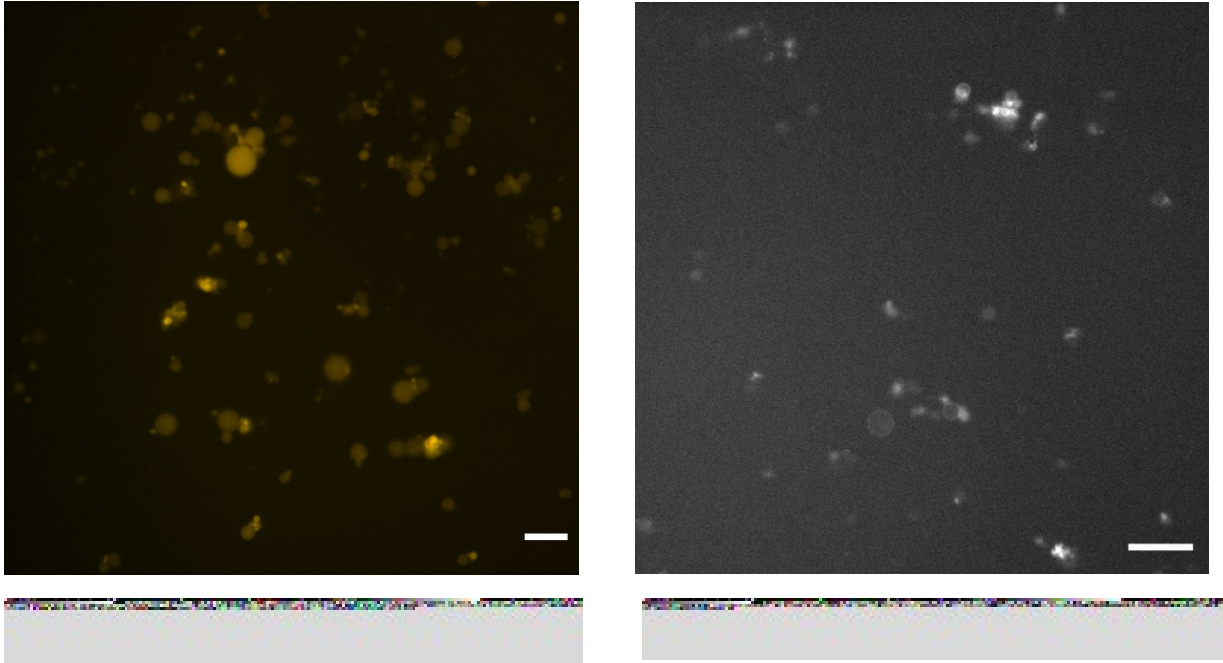
Full fields of view for the experiment displayed in Figure 4; after HCl addition (pH 5.5).



Micrographs of the fluorescent signal from the pH probe (left) and bioluminescent signal from the reconstituted NanoBiT (right). The GUVs contained 2% DOGS-NTA-Ni, 5 μ M LgBiT, 5 μ M SmBiT, 100 U/ml urease and 0.1 mg/ml dextran-FT (pH probe) and were prepared at pH 7.5. Addition of HCl to the external medium decreased the pH to 5.5 and attenuated the bioluminescent signal. Scale bar represents 50 μ m.

Supplementary Figure 13.

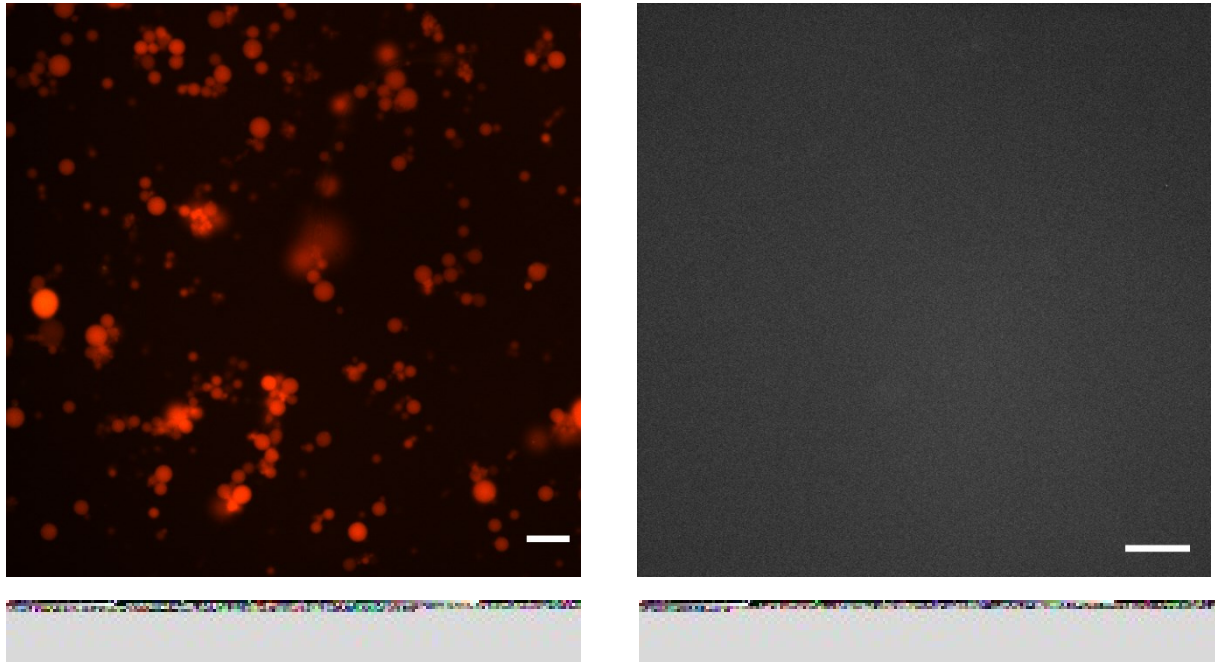
Full fields of view for the experiment displayed in Figure 4; after urea addition.



Micrographs of the fluorescent signal from the pH probe (left) and bioluminescent signal from the reconstituted NanoBiT (right). The GUVs contained 2% DOGS-NTA-Ni, 5 μ M LgBiT, 5 μ M SmBiT, 100 U/ml urease and 0.1 mg/ml dextran-FT (pH probe) and were prepared at pH 7.5. After addition of HCl to the external medium the pH decreased to 5.5. Next, either urea (40 mM) or water was added to the external medium. The conversion of urea by encapsulated urease and the concomitant pH increase were tracked by recording the fluorescence from the pH probe in the lumen of the vesicles. These micrographs display the signal from the pH probe and the restoration of bioluminescence 110 min after urea addition for different positions in the sample. Scale bars represent 50 μ m.

Supplementary Figure 14.

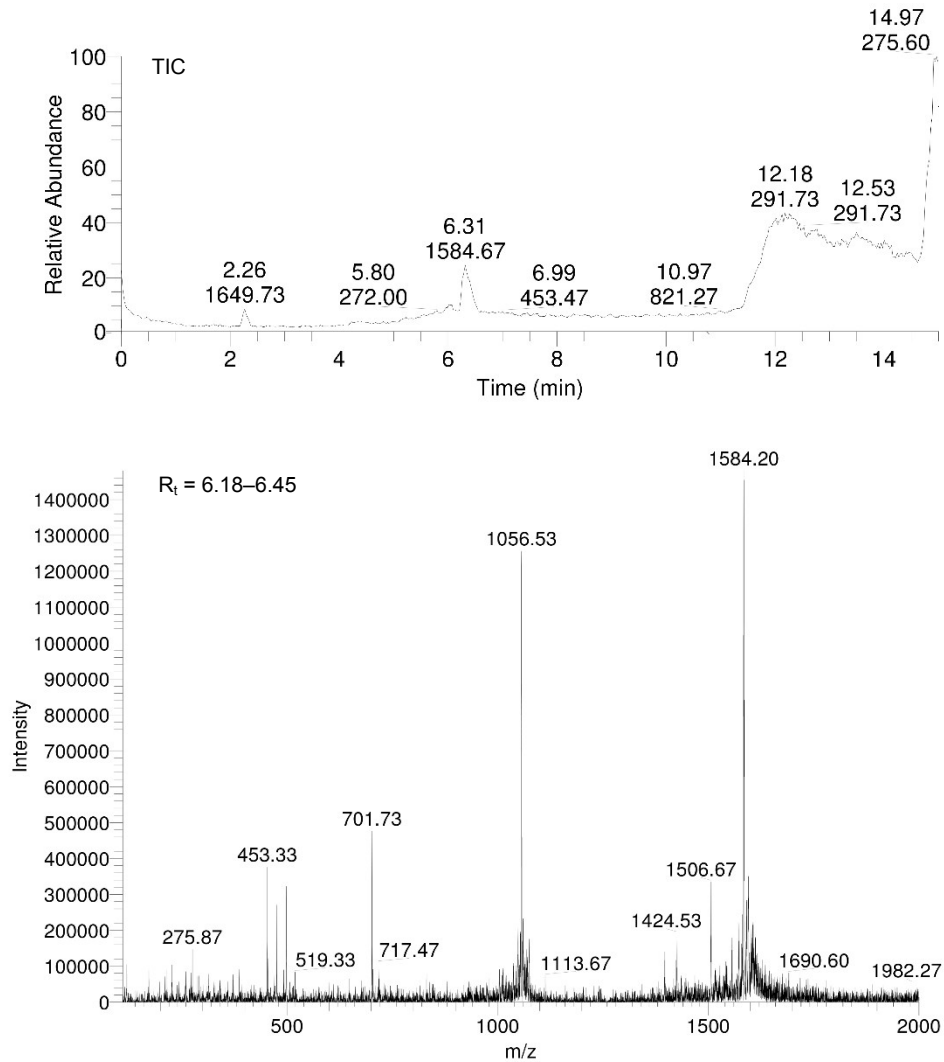
Full fields of view for the experiment displayed in Figure 4; no urea added.



As in **Suppl. Fig. 13**, but here urea was not added to the external medium, and restoration of neither pH nor bioluminescence was observed.

Supplementary Figure 15.

His-SmBiT LC-MS chromatogram.

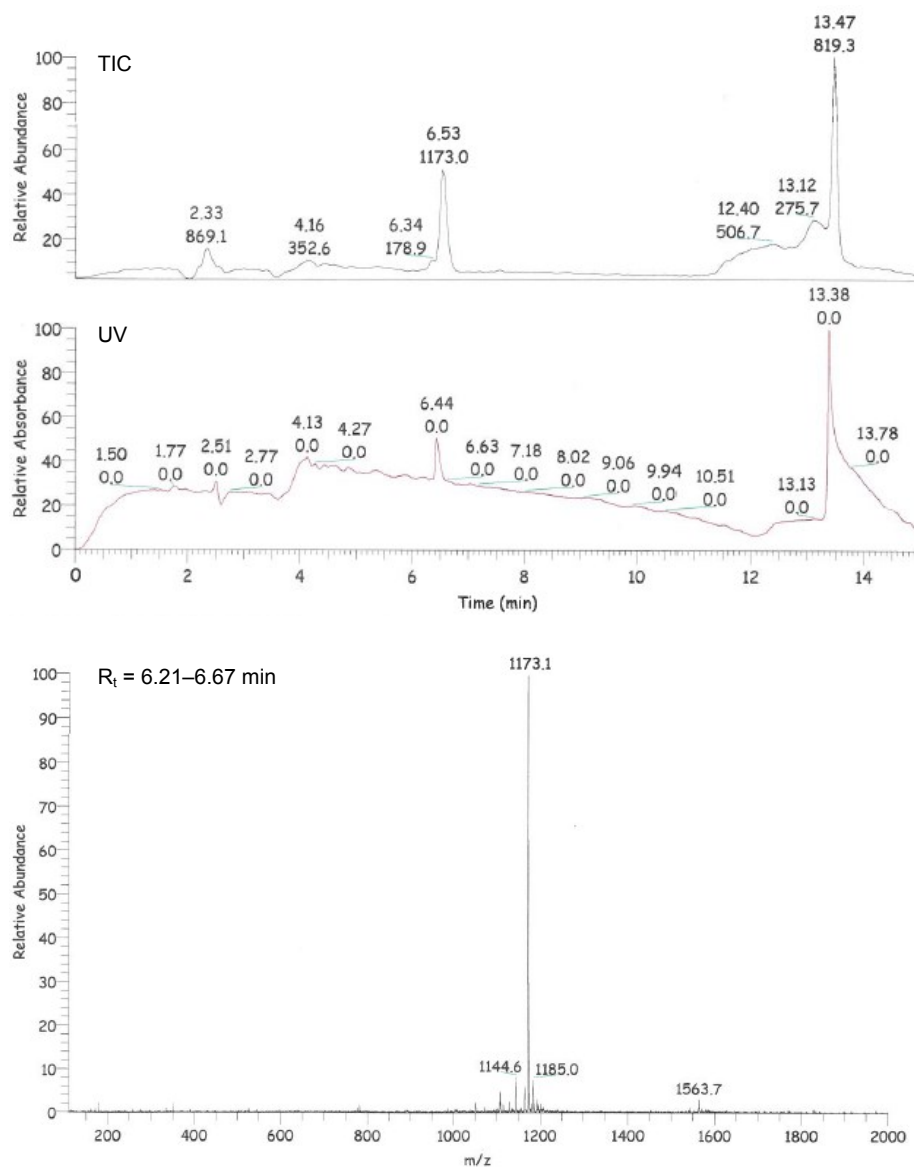


H-HHHHHHGGSGGGGSGGSSGGVTGYRLFEEIL-NH₂

C₁₃₄H₁₉₆N₄₈O₄₃ Calculated: 1584.2, found: 1584.2 [M+2H]²⁺; calculated: 1056.5, found: 1056.5 [M+3H]³⁺

Supplementary Figure 16.

NOHis-SmBiT LC-MS chromatogram.

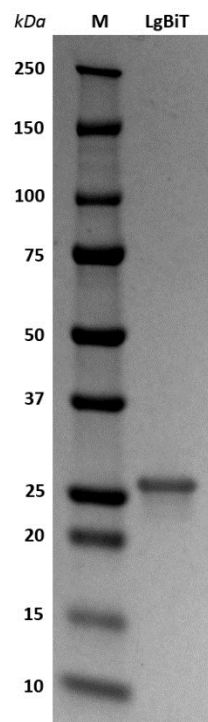


H-GGSGGGGSGSSSGVVTGYRLFEEIL-NH₂

C₉₈H₁₅₄N₃₀O₃₇: calculated: 1173.1, found: 1173.1 [M+2H]²⁺

Supplementary Figure 17.

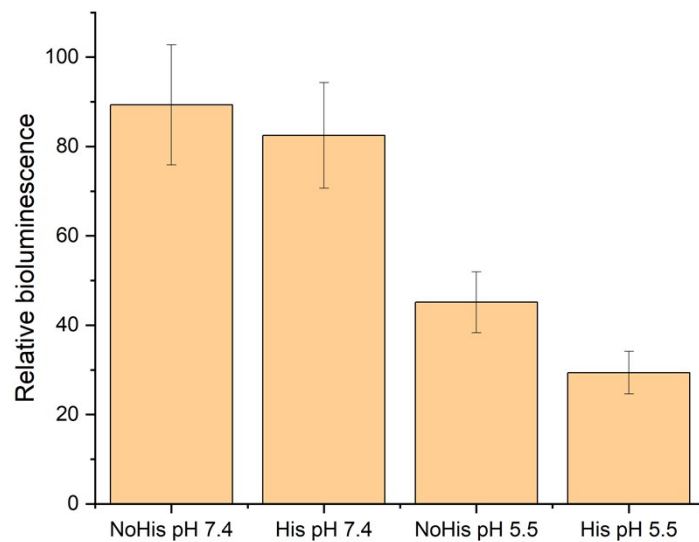
SDS-PAGE analysis of purified LgBiT



Analysis of the purified recombinant protein by SDS-PAGE (4-20% Mini-PROTEAN TGX Precast Protein Gel, Bio-Rad). M = Marker (Precision Plus Protein™ Dual Color Standards, Bio-Rad); LgBiT = purified His₆-LargeBiT-GGS₁₀-CT52 (theoretical MW = 27 kDa).¹

Supplementary Figure 18.

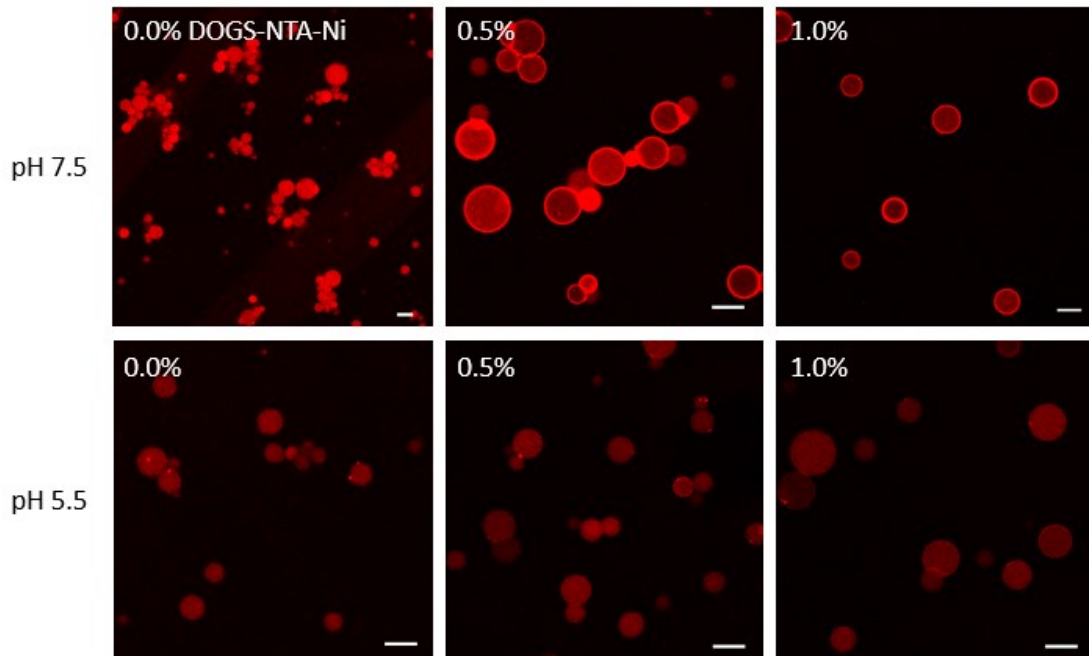
Effect of the His-tag and pH on luciferase activity



Relative bioluminescence in bulk solutions containing LgBiT (5 μ M) and either His-SmBiT or NoHis-SmBiT (5 μ M), at pH 7.4 and at pH 5.5. Buffer composition was 10 mM K_2HPO_4 , 300 mM NaCl. The Nano-Glo substrate was diluted 1:50. Error bars denote the standard deviations.

Supplementary Figure 19.

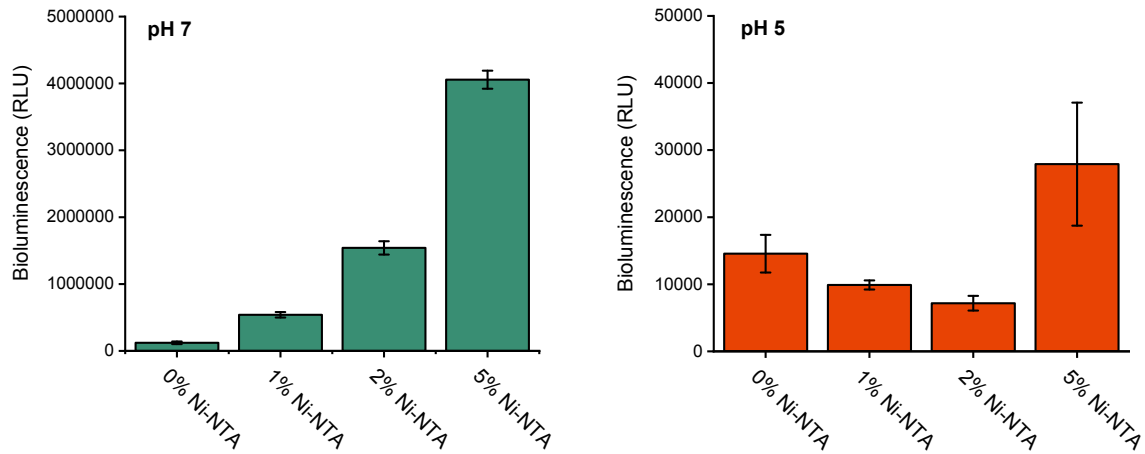
Direct visualization of His-tagged protein distribution using fluorescent tdTomato



To directly visualize the pH-responsive binding of His-tagged proteins to the Ni-NTA moieties at the liposomal membrane, and since LgBiT and SmBiT fragments are not fluorescent, we used another His-tagged protein – tdTomato. As tdTomato is fluorescent at both pH 7 and 5, its distribution inside the liposomes could be evaluated utilizing a pH-independent read-out. Indeed, these data showed that at pH 7.5 the His-tagged protein was bound to the liposomal membrane, whereas at pH 5.5 it is distributed homogeneously throughout the vesicle. As both the immobilization of tdTomato and the luciferase fragments rely on His-tag/Ni-NTA interactions, we can reasonably assume that both luciferase fragments show similar pH-dependent distributions. GUVs contained 2.5 μ M tdTomato. Scale bars represent 15 μ m.

Supplementary Figure 20.

Dependency of the total luciferase activity on Ni-NTA concentration at different pH values

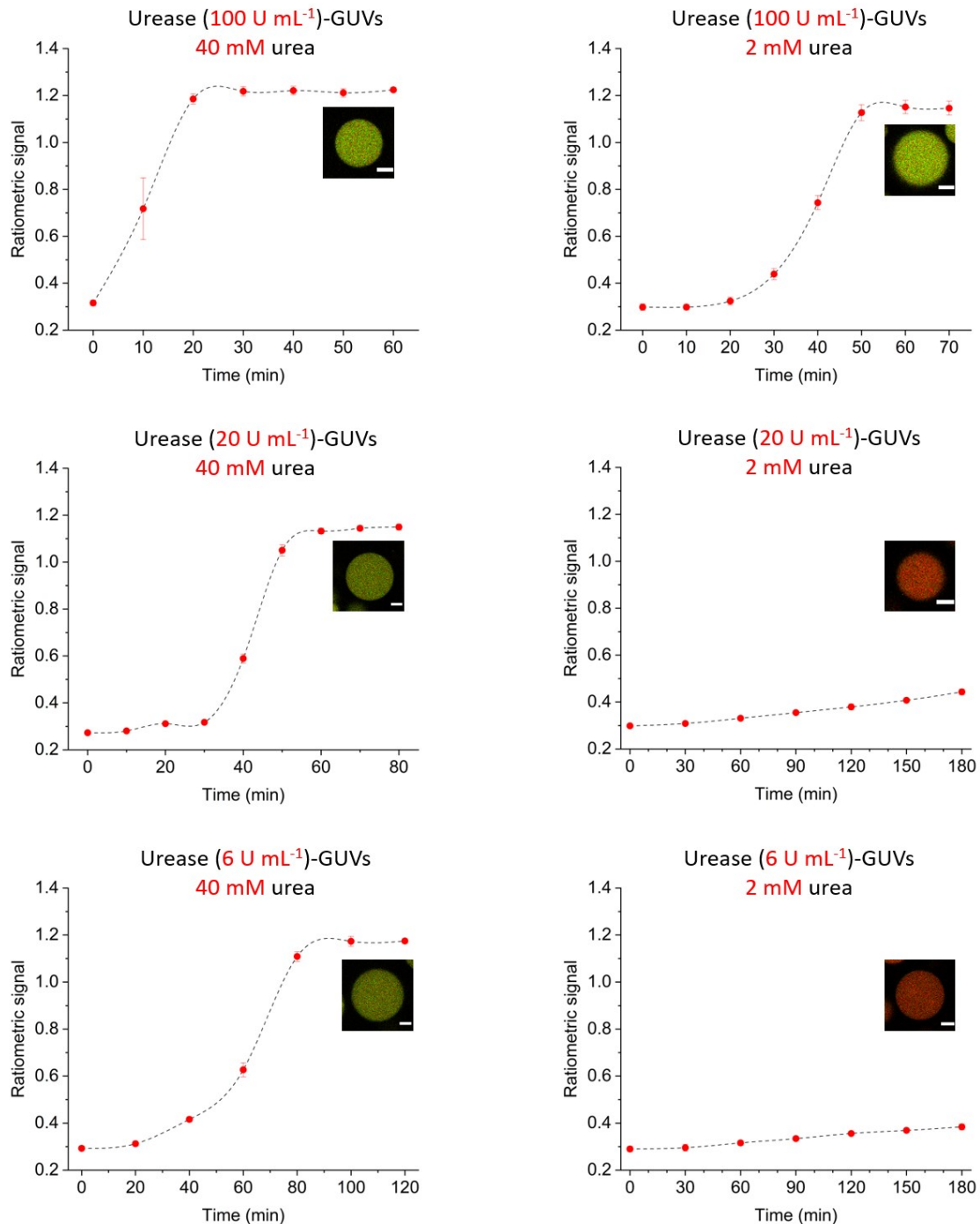


As shown for tdTomato, His-tagged proteins dissociate from the liposomal membrane at pH 5.5. Although this dissociation could not be observed directly for the luciferase fragments, we could investigate the effect of the Ni-NTA moieties on the total luciferase activity at pH 7 and pH 5. This showed that at pH 7 the total activity is dependent on the concentration of Ni-NTA in the membrane, indicating fragment recruitment at the membrane. In contrast, at pH 5 the activity was equivalent for GUVs displaying Ni-NTA on their membrane or GUVs that did not contain Ni-NTA – thus, further indicating no significant membrane association at acidic pH.

GUVs were prepared at pH 7 and incubated with 50 nM LgBiT & His-SmBiT. First, the bioluminescence at pH 7 was recorded directly after addition of furimazine (1:1000 final dilution). Next, the pH of the solution was set to 5 using dilute HCl and the bioluminescence was recorded using a fresh aliquot of furimazine.

Supplementary Figure 21.

Dynamics of the pH-responsive, ratiometric signal depending on the amount of encapsulated urease and urea in the environment



Urease-loaded GUVs were prepared as described above on page 5 but containing different amounts of urease. After 20 min incubation in the presence α HL (20 μ g/ml, urea was added at a high (40 mM) or a low (2 mM) concentration. The experiments were initiated at pH 5.5. The ratiometric signal of the co-encapsulated pH-probe (dextran-fluorescein-tetramethylrhodamine) was then monitored in order to investigate the dynamics of the pH of the system. GUVs containing 100 U mL⁻¹ of urease – which correspond to the amount employed in luciferase

reconstitution experiments (Figure 4) – could quickly increase their internal pH at 40 mM and at 2 mM of urea in less than 1 h. At 40 mM urea, the GUVs with 20 and 6 U mL⁻¹ also could upregulate their internal pH but with slower kinetics (note the different time scales). Interestingly, the GUVs with 20 or 6 U mL⁻¹ showed a negligible response to the low urea concentration (2 mM) even after 3 hours. The ratiometric signal corresponds to the ratio between fluorescein and rhodamine channels – at least 5 GUVs were analyzed per data point. Insets display micrographs of overlaid confocal channels; yellow color indicating deacidification of the lumen, red color corresponding to an acidic environment.

Supplementary references

- (1) Aper, S. J. A.; den Hamer, A.; Wouters, S. F. A.; Lemmens, L. J. M.; Ottmann, C.; Brunsveld, L.; Merkx, M. Protease-Activatable Scaffold Proteins as Versatile Molecular Hubs in Synthetic Signaling Networks. *ACS Synth. Biol.* **2018**, *7* (9), 2216–2225.
- (2) Peters, R. J. R. W.; Nijemeisland, M.; van Hest, J. C. M. Reversibly Triggered Protein-Ligand Assemblies in Giant Vesicles. *Angew. Chem. Int. Ed.* **2017**, *54*, 13258-13262.
- (3) Pautot, S.; Frisken, B. J.; Weitz, D. A. Production of Unilamellar Vesicles Using an Inverted Emulsion. *Langmuir* **2003**, *19* (7), 2870–2879.
- (4) <http://questpharma.u-strasbg.fr/html/radial-profile-ext.html>